

Supplementary material for the paper: “Frictionless motion of lattice defects”

N. Gorbushin,¹ G. Mishuris,² and L. Truskinovsky¹

¹*PMMH, CNRS – UMR 7636, CNRS, ESPCI Paris, PSL Research University, 10 rue Vauquelin, 75005 Paris, France*

²*Department of Mathematics, Aberystwyth University, Ceredigion SY23 3BZ, Wales, UK*

(Dated: September 24, 2020)

FPU PROBLEM: ANALYTICAL SOLUTION

In this problem the characteristic function $L(k)$ has the following properties: $L(-k) = L(k)$ and $L(\bar{k}) = \overline{L(k)}$ and, hence, the real and purely imaginary roots of the characteristic equation $L(k) = 0$ come in pairs while other complex roots come in quadruplets. Therefore, it is enough to search for the roots of the characteristic equation in the quarter of the complex plane $\text{Im } k \geq 0$ and $\text{Re } k \geq 0$. The associated roots can be conveniently sorted between the sets $Z^\pm = Z_c^\mp \cup Z_r^\pm$ with $Z_c^\pm = \{k : L(k) = 0, \pm \text{Im } k > 0\}$ and $Z_r^\pm = \{|k| > 0 : L(k) = 0, \text{Im } k = 0, \pm k L'(k) > 0\}$, see Fig. 1.

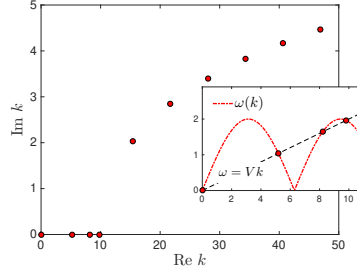


Figure 1: Real and complex roots $L(k) = 0$ for the FPU problem. The inset shows the dispersion relation.

With the roots known, the integration in Eq. 2 in the main text can be performed explicitly which allows one to obtain the expression for the full strain field:

$$\varepsilon(\eta) = \begin{cases} \varepsilon_+ + \sum_{j=1}^K A_j \sin(k_j \eta + \varphi_j) - \sum_{k_j \in Z^+} \frac{\sigma_0 \omega^2(k_j)}{k_j L'(k_j)} e^{-ik_j \eta}, & \eta > 0, \\ \varepsilon_- + \sum_{j=1}^K A_j \sin(k_j \eta + \varphi_j) + \sum_{k_j \in Z^-} \frac{\sigma_0 \omega^2(k_j)}{k_j L'(k_j)} e^{-ik_j \eta}, & \eta < 0, \end{cases} \quad (\text{S1})$$

To use the switching condition $\varepsilon(0) = \varepsilon_c$, we need to recall the following general properties of the roots of the characteristic equation [1]

$$\sum_{k_j \in Z_c^+} \frac{\omega^2(k_j)}{k_j L'(k_j)} + \sum_{k_j \in Z_c^-} \frac{\omega^2(k_j)}{k_j L'(k_j)} = -\frac{1}{1-V^2} - \sum_{k_j \in Z_r^+} \frac{\omega^2(k_j)}{k_j L'(k_j)} - \sum_{k_j \in Z_r^-} \frac{\omega^2(k_j)}{k_j L'(k_j)}, \quad (\text{S2})$$

$$\sum_{k_j \in Z_c^+} \frac{\omega^2(k_j)}{k_j L'(k_j)} = \sum_{k_j \in Z_c^-} \frac{\omega^2(k_j)}{k_j L'(k_j)}. \quad (\text{S3})$$

We can rewrite the switching condition in two equivalent forms $\varepsilon_\pm = \varepsilon_c \mp \frac{\sigma_0/2}{1-V^2} + \sigma_0 Q + \sum_{j=1}^K A_j \sin \varphi_j$, where

$$Q = \frac{1}{2} \sum_{k_j \in Z_r^+} \frac{\omega^2(k_j)}{k_j L'(k_j)} - \frac{1}{2} \sum_{k_j \in Z_r^-} \frac{\omega^2(k_j)}{k_j L'(k_j)}. \quad (\text{S4})$$

Next, we compute the rate of dissipation by lattice waves:

$$\mathcal{R}_\pm = \sum_{k_j \in Z_r^\mp} \langle \mathcal{E}_j \rangle |\omega'(k_j) - V|, \quad (\text{S5})$$

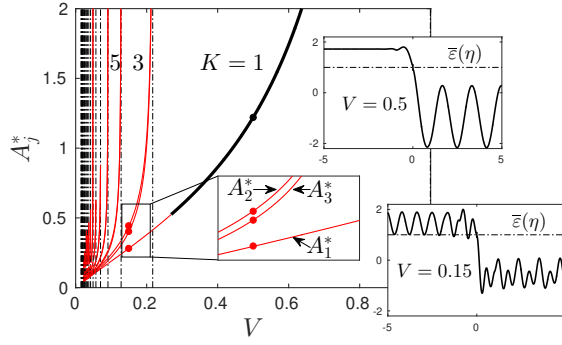


Figure 2: Amplitudes of the AC sources $A_j^*(V)$, $j = 1, 2, \dots, K$ for $K = 1, 3, 5, \dots$; insets show strains $\bar{\varepsilon}(\eta) = \varepsilon(\eta)/\varepsilon_c$ at $V = 0.15$ and $V = 0.5$ with corresponding A_j^* marked by solid circles. Black lines correspond to admissible solutions, red - to non admissible. Parameters: $\sigma_0 = 2$, $\varepsilon_c = 1$.

where $\mathcal{E}_j = v_j^2/2 + w(\varepsilon_j)$ is the energy density carried by the linear wave with the (real) wave number $k_j > 0$ and $\omega'(k_j) - V$ is the velocity of the energy drift relative to the velocity of the defect; the signs indicate waves carrying the energy to $\pm\infty$. The particle velocity here $v(\eta) = -V du/d\eta$ can be obtained by inverting the kinematic relation in the Fourier space $\hat{v}(k) = -Vk \exp(ik/2)/[2 \sin(k/2)]\hat{\varepsilon}(k)$. We obtain explicitly:

$$v(\eta) = \begin{cases} -V\varepsilon_+ - \sum_{j=1}^K \frac{A_j V k_j}{2 \sin(k_j/2)} \sin(k_j(\eta - 1/2) + \varphi_j) + \sum_{k_j \in Z^+} \frac{\sigma_0 V k_j \omega^2(k_j)}{2k_j \sin(k_j/2) L'(k_j)} e^{-ik_j(\eta-1/2)}, & \eta > 1/2, \\ -V\varepsilon_- - \sum_{j=1}^K \frac{A_j V k_j}{2 \sin(k_j/2)} \sin(k_j(\eta - 1/2) + \varphi_j) - \sum_{k_j \in Z^-} \frac{\sigma_0 V k_j \omega^2(k_j)}{2k_j \sin(k_j/2) L'(k_j)} e^{-ik_j(\eta-1/2)}, & \eta < 1/2. \end{cases} \quad (S6)$$

After the substitution we obtain

$$G_{\pm} = \frac{\mathcal{R}_{\pm}}{V} = \sum_{k_j \in Z_r^{\pm}, k_j > 0} \left[\left(\pm 2 \frac{\sigma_0 \omega^2(k_j)}{k_j L'(k_j)} - A_j \sin \varphi_j \right)^2 + A_j^2 \cos^2 \varphi_j \right] \left| \frac{\omega'(k_j)}{V} - 1 \right|. \quad (S7)$$

The first term in the square parenthesis reveals the interaction between the waves generated by AC forces and the waves radiated by the defect. The second term corresponds to the contribution from the AC sources only. If we use the definitions of G^M , Eq. 4, and G^m , Eq. 5, in the main text and substitute the expressions of the fields $\varepsilon(\eta)$ and $v(\eta)$, we obtain the relation

$$G = G^M + G^m = G_+ + G_-. \quad (S8)$$

To verify this identity it is enough to observe that $2\omega^2(k_j)/(k_j L'(k_j)) = V/(\omega'(k_j) - V)$.

In the presence of AC driving the rate of dissipation G depends not only on the velocity of the defect V but also on the parameters of the AC sources A_j and φ_j where $j = 1, \dots, K$. In the simplest case of a single source we obtain $G = \sigma_0^2 Q - \sigma_0 A_1 \sin \varphi_1 + (1/2) A_1^2 |\omega'(k_1)/V - 1| = G(V, A_1, \varphi_1)$. Here the dependence on the phase shift φ_1 is periodic and bounded and we can conclude that each choice of V and A_1 generates an *interval* of G s (which reduces to a point when $A_1 = 0$). The generic structure of the resulting *kinetic domain* at a particular $A_1 \neq 0$ is depicted in Fig.2 of the main text where we only show admissible solutions.

From the representation (S7) it is now straightforward to conclude that the condition $G^M + G^m = 0$ is satisfied if we set $\varphi_j = \varphi_j^* = \pi/2$ and choose amplitudes $A_j = A_j^* = (-1)^j \sigma_0 V / (\omega'(k_j) - V)$, $j = 1, 2, \dots, K$, see Fig. 2.

FPU PROBLEM: NUMERICAL SOLUTION

To show how the DC and AC driving can be actually implemented and to show stability of the obtained analytical solutions we we conducted a series of direct numerical experiments with a finite chain comprised of $N = 1001$ masses connected by bi-stable springs.

Our initial conditions contained a pre-existing defect (phase boundary) located at $n_0 = 200$. We assigned initial displacements (linear with j) in the form $u_j(0) = \tilde{\varepsilon}_- j$ for $j \leq n_0$ and $u_j(0) = \tilde{\varepsilon}_- n_0 + \tilde{\varepsilon}_+(j - n_0)$ for $j > n_0$, where $\tilde{\varepsilon}_{\pm} = \varepsilon_c \mp \sigma_0/2 + \varepsilon_+ - A/2$. Here and below, constants ε_{\pm} correspond to the limiting strains and A is an amplitude of the AC drive which we use in the analytical solution. The initial velocities are set to 0 for each mass: $\dot{u}_j(0) = 0$.

We fix the end of the chain on the right side by setting: $u_{N+1}(t) = u_N(0) + \bar{\varepsilon}_+$. The left end is loaded by a constant force $F = \sigma(\varepsilon_-) + \sigma_0 V / (2(1 + V))$ representing the DC driving so that: $\ddot{u}_1(t) = \sigma(u_1 - u_2) - FH(t - t_0)$.

The time shift t_0 is needed for the energy from the AC source to arrive to the defect located at $n = n_0$. We associate the AC driving source with the two neighboring masses $j_0 = 400$ and $j_0 + 1$ which are located sufficiently far ahead of the initial defect and the right end of a chain. More specifically, we assume that a time periodic pair of force is applied to the spring located between these masses ensuring that the strain in this spring remains the same all the time. The resulting system of equations can be written in the form:

$$\ddot{u}_j(t) = \sigma(u_{j+1} - u_j) - \sigma(u_j - u_{j-1}) - A(\delta_{jj_0} + \delta_{j(j_0+1)}) \sin(\nu t), \quad (\text{S9})$$

where δ_{ij} is the Kronecker delta, $\nu = k_1 V$ and k_1 is the first real positive root of the equation $L(k) = 0$.

We performed simulations with 100 transition events taking place before the waves reflected from the boundaries of the chain took any effect. The defect was shown to approach the steady-state TW regime for several values of velocity V which suggests that the corresponding analytical solution is a dynamic attractor.

Our Fig. 3 shows time evolution of the strain field. The insets in Fig. 3(c) show comparison between the numerically obtained data and the analytical solution for $A = 0.6$, $V = 0.45$ and $\varepsilon_- = 2.21$. In this case $\varepsilon_+ = -0.29$ and $G^M + G^m = 0.27$ (the other parameters are $\sigma_0 = 2$, $\varepsilon_c = 1$). The calculations were made with the ode45 solver of MATLAB.

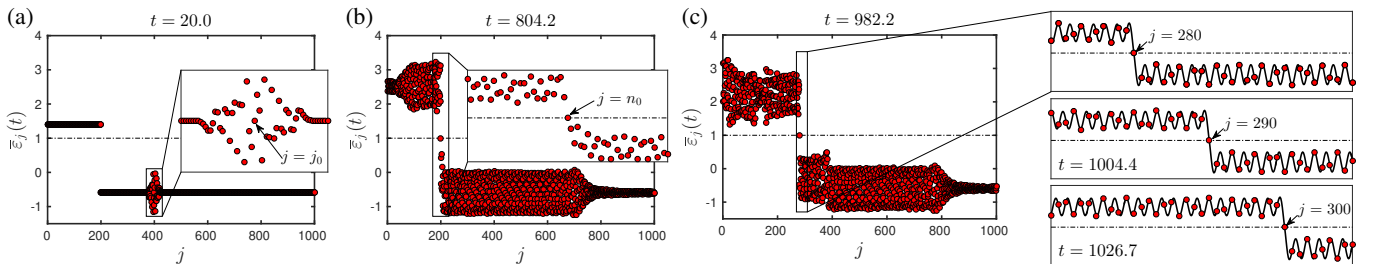


Figure 3: Snapshots of the normalized strains $\bar{\varepsilon}_j(t) = \varepsilon_j(t)/\varepsilon_c$ at different moments: (a) initial propagation of the wave from the AC forces centred at $j = j_0 = 400$ and $j_0 + 1$; the initial defect is at $j = n_0 = 200$; (b) the first transition event takes place at $j = n_0$ soon after the energy from the DC force (turned on at $t = t_0 = 600$) at the left end arrived; (c) steady-state propagation achieved when the comparison with the analytical solution (black solid lines) is possible; the insets on the right show snapshots of strains when the front is at $j = 280, 290$ and 300 .

In the attached Movie 2 we show the dynamic propagation of the phase boundary as demonstrated in the insets of Fig. 3(c). The numerical solution is interposed with the analytical solution of the front moving at $V = 0.45$. During the propagation of the defect, the points progressively move from the phase with ε_+ to the phase with ε_- by passing ε_c . The trajectories follow precisely the analytical solution. To complement the animation we show in Fig. 4 the direct comparison of numerical and analytical deformation histories in a generic location. The analytical solution, known as a function of $\eta = n - Vt$, was re-scaled to be compared with the numerically obtained field $\varepsilon_n(t)$ corresponding to steady state.

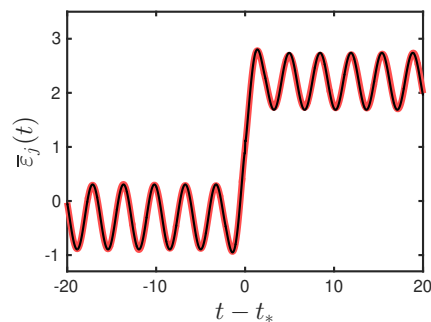


Figure 4: Perfect overlap of the normalized steady state strain history $\bar{\varepsilon}_j(t) = \varepsilon_j(t)/\varepsilon_c$ obtained in the simulation shown in Fig. 3 for $j = 290$ (red line) with the corresponding analytical solution (black line). Time t_* marks the transition event.

FPU PROBLEM: SPINODAL REGION

Suppose now that the FPU potential is C^1 smooth and tri-parabolic which implies that it incorporates a spinodal region where the elastic modulus of the connecting springs is negative. More specifically, we consider the dimensionless stress-strain relation $\sigma(\varepsilon)$ of the form

$$\sigma(\varepsilon) = \begin{cases} \varepsilon, & \varepsilon < \varepsilon_c, \\ -(\sigma_0/\delta)(\varepsilon - \varepsilon_c) + \varepsilon_c, & \varepsilon_c \leq \varepsilon \leq \varepsilon_c + \delta, \\ \varepsilon - (\delta + \sigma_0), & \varepsilon > \varepsilon_c + \delta. \end{cases} \quad (\text{S10})$$

Here the width of the spinodal region is denoted by δ while the other notations are the same as in the main paper.

Following [2, 3], we search for the TW solutions in the form:

$$\sigma(\eta) = \varepsilon(\eta) - \int_{-z}^0 w(s)H(s - \eta)ds, \quad \int_{-z}^0 w(s)ds = \delta + \sigma_0, \quad (\text{S11})$$

where z determines the spacial width of the spinodal zone and $w(\eta)$ is a new unknown function. The continuity of the strain should be now enforced in two points: $\varepsilon(0) = \varepsilon_c$ and $\varepsilon(-z) = \varepsilon_c + \delta$.

If the function $w(\eta)$ is known, we can again use the Fourier transform to obtain

$$\varepsilon(\eta) = \varepsilon_{dr}(\eta) + \frac{1}{2\pi} \int_{-\infty}^{\infty} \frac{\omega^2(k)}{(0 + ik)L(k)} W(k) e^{-ik\eta} dk, \quad W(k) = \int_{-z}^0 w(s) e^{iks} ds. \quad (\text{S12})$$

Here the dispersion relation $\omega(k)$ and the kernel $L(k)$ are the same as in the main text. The action of applied loads is again represented by the term $\varepsilon_{dr}(\eta)$ satisfying the condition $L(k)\hat{\varepsilon}_{dr}(k) = 0$. To model the simplest external AC source we can choose again $\varepsilon_{dr}(\eta) = A_1 \sin(k_1\eta + \varphi_1) + C$.

To find the equation for the function $w(\eta)$ we need to first differentiate (S12) to obtain

$$\varepsilon'(\eta) = \varepsilon'_{dr}(\eta) - \int_{-z}^0 w(s)q(\eta - s)ds, \quad q(\eta) = \frac{1}{2\pi} \int_{-\infty}^{\infty} \frac{\omega^2(k)}{L(k)} e^{-ik\eta} dk \quad (\text{S13})$$

where the prime is the derivative with respect to η . On the other hand we know from (S11) that $\sigma'(\eta) = \varepsilon'(\eta) + w(\eta)$ and from (S10) that $\sigma'(\eta) = -(\sigma_0/\delta)\varepsilon'(\eta)$ when $-z < \eta < 0$. This allows us to eliminate $\varepsilon'(\eta)$ from (S13) and obtain the desired equation for $w(\eta)$

$$w(\eta) = \left(1 + \frac{\sigma_0}{\delta}\right) \left[\int_{-z}^0 w(s)q(\eta - s)ds - \varepsilon'_{dr}(\eta) \right], \quad -z < \eta < 0, \quad (\text{S14})$$

which must be supplemented by the normalization condition $\int_{-z}^0 w(s)ds = \delta + \sigma_0$ allowing one to find the value of z .

Finally, to find the constant C we need to use the only remaining matching condition at $\eta = 0$. The solution $\varepsilon(\eta)$ can be equivalently written as

$$\varepsilon(\eta) = \varepsilon_{dr}(\eta) + \int_{-z}^0 w(s)\varepsilon_0(\eta - s) ds, \quad \varepsilon_0(\eta) = \frac{1}{2\pi} \int_{-\infty}^{\infty} \frac{\omega^2(k)}{(0 + ik)L(k)} e^{-ik\eta} dk \quad (\text{S15})$$

where the term $\varepsilon_0(\eta)$ corresponds to $\varepsilon_{in}(\eta)$ with $\sigma_0 = 1$ in the main text of the paper. We define again the far field states for $\varepsilon_0(\eta)$ obtaining $\varepsilon_0^+ = 0$ and $\varepsilon_0^- = 1/(1 - V^2)$. Taking the limit and using the normalization condition we obtain

$$\varepsilon_{\pm} = \langle \varepsilon_{dr} \rangle (\pm\infty) + \varepsilon_0^{\pm} (\sigma_0 + \delta) \quad (\text{S16})$$

where $\varepsilon_{\pm} = \langle \varepsilon(\eta) \rangle (\pm\infty)$. We conclude that again $C = \varepsilon_+$ but now $\varepsilon_- = \varepsilon_+ + (\sigma_0 + \delta)/(1 - V^2)$. Imposing the continuity at $\eta = 0$ we obtain

$$C = \varepsilon_c - A_1 \sin \varphi_1 - \int_{-z}^0 w(s)\varepsilon_0(-s) ds \quad (\text{S17})$$

We note that the condition $\varepsilon(-z) = \delta + \sigma_0$ is ensured by the imposed normalization condition on $w(\eta)$. The admissibility condition in this case becomes

$$\begin{cases} \varepsilon(\eta) < \varepsilon_c, & \eta > 0, \\ \varepsilon_c < \varepsilon(\eta) < \varepsilon_c + \delta, & -z < \eta < 0, \\ \varepsilon(\eta) > \varepsilon_c + \delta, & \eta < -z \end{cases} \quad (\text{S18})$$

For our purposes here it was sufficient to solve the linear integral equation (S14) numerically using the collocation method. As in the case $\delta = 0$ considered in the main part of the paper, for each set of the parameters V and A_1 we find a one parametric family of admissible solutions depending on the value of the phase shift φ_1 .

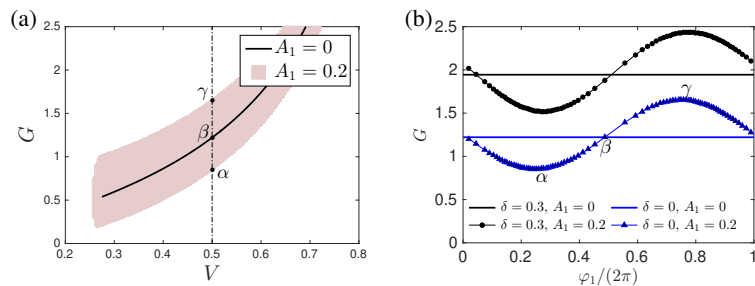


Figure 5: (a) The rate of dissipation $G(V)$ for the case $K = 1$ and $\delta = 0$ (no spinodal region). Points α and γ mark minimum and maximum of G when $\delta = 0$ and $V = 0.5$. (b) The rate of dissipation as a function of φ_1 at two values of A_1 and $V = 0.5$ for $\delta = 0$ and $\delta = 0.3$. Other parameters are $\sigma_0 = 2$, $\varepsilon_c = 1$.

To illustrate these solutions we generalize for the case $\delta > 0$ the formula for the macroscopic energy release rate $G^M = 0.5(\sigma_0 + \delta)(\varepsilon_+ + \varepsilon_- - 2\varepsilon_c) + 0.5(\sigma_0 - 2\varepsilon_c)\delta$, while noting that the expression for G^m remains unchanged. In Fig. 5(b) we show the rate of dissipation for admissible solutions $G(\varphi_1) = G^M(\varphi_1) + G^m(\varphi_1)$ at $V = 0.5$ and $A_1 = 0.2$. We obtain the same trends as in the case $\delta = 0$, in particular, we see that AC driving can lower the friction. The study of the zero friction solutions for the case $\delta > 0$ will be presented separately.

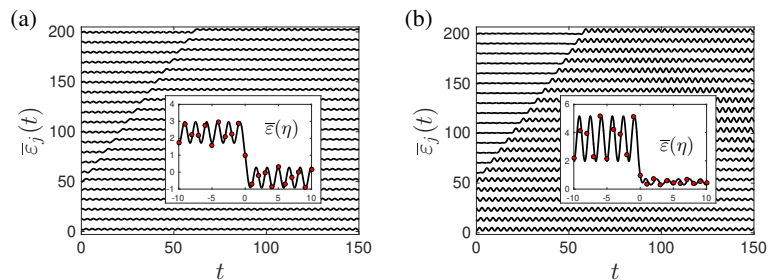


Figure 6: Normalized strain histories $\bar{\varepsilon}_j(t) = \varepsilon_j(t)/\varepsilon_c$ for $j = 240, 282, \dots, 290$: (a) $\delta = 0$ and (b) $\delta = 0.3$. The insets show the comparison of the analytical solutions (solid lines) with the numerically reached steady states at $t = 40$ (red markers).

In Fig. 6 we illustrate stability of the obtained analytical solutions. We solved numerically the FPU system with 500 springs and initial data approximating the analytical solution with the lowest value of G in Fig. 5: the random perturbations of the initial strain field were drawn from the uniform distribution on the interval $[-0.1, 0.1]$. The initial location of the front was at $n_0 = 250$. Our Fig. 6 shows convergence to the expected TW solutions in both cases, $\delta = 0$ (no spinodal region) and $\delta = 0.3$.

FK PROBLEM: ANALYTICAL SOLUTION

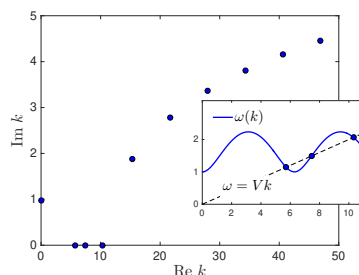


Figure 7: Real and complex roots $L(k) = 0$ for the FK problem. The inset shows the dispersion relation.

By performing integration in Eq. 7 in the main text we obtain the expression for the displacement field

$$u(\eta) = \begin{cases} u_+ + \sum_{j=1}^K A_j \sin(k_j \eta + \varphi_j) - \sum_{k_j \in Z^+} \frac{\sigma_0}{k_j L'(k_j)} e^{-ik_j \eta}, & \eta > 0, \\ u_- + \sum_{j=1}^K A_j \sin(k_j \eta + \varphi_j) + \sum_{k_j \in Z^-} \frac{\sigma_0}{k_j L'(k_j)} e^{-ik_j \eta}, & \eta < 0. \end{cases} \quad (\text{S19})$$

The sets Z^\pm are defined in the same way as in the FPU problem and demonstrated in Fig. 7.

The switching condition $u(0) = u_c$ can be again written in two equivalent forms $u_\pm = u_c \mp (\sigma_0/2) + \sigma_0 R - \sum_j A_j \sin \varphi_j$, where

$$R = \frac{1}{2} \sum_{k_j \in Z_r^+} \frac{1}{k_j L'(k_j)} - \frac{1}{2} \sum_{k_j \in Z_r^-} \frac{1}{k_j L'(k_j)}. \quad (\text{S20})$$

Next we compute the rate of energy dissipation $\mathcal{R}_\pm = G_\pm V$ following the same methodology as in the FPU problem. We obtain:

$$G_\pm = \sum_{k_j \in Z_r^\pm, k_j > 0} \left[\left(\pm 2 \frac{\sigma_0}{k_j L'(k_j)} - A_j \sin \varphi_j \right)^2 + A_j^2 \cos^2 \varphi_j \right] \omega^2(k_j) \left| \frac{\omega'(k_j)}{V} - 1 \right|. \quad (\text{S21})$$

The energy balance (S8) remains the same and can be again verified by direct substitution. From (S21) one can see that the choice $\varphi_j = \varphi_j^* = \pi/2$ and $A_j = A_j^* = (-1)^j \sigma_0 V / (\omega(k_j)^2 (\omega'(k_j) - V))$, $j = 1, 2, \dots, K$ ensures frictionless propagation of the defect. The velocity dependence of A_j^* for $K > 1$ is illustrated in Fig. 8.

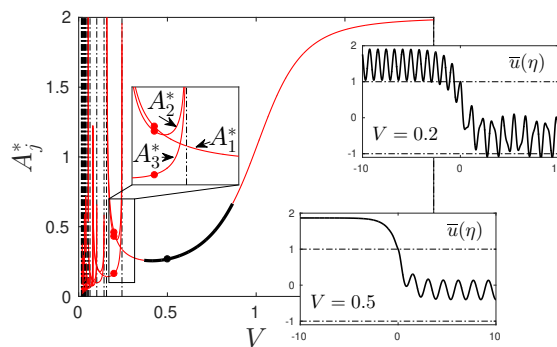


Figure 8: Amplitudes of the AC sources in FK problem: $A_j^*(V)$, $j = 1, 2, \dots, K$ for $K = 1, 3, 5, \dots$. Insets show strains $\bar{u}(\eta) = u(\eta)/u_c$ at $V = 0.2$ and $V = 0.5$ with corresponding A_j^* marked by solid circles. Black lines correspond to admissible solutions, red - to non admissible. Parameters: $\sigma_0 = 2$, $u_c = 1$.

PB PROBLEM: ANALYTICAL SOLUTION

With the TW ansatz applied, the Fourier transform reduces Eq. 11 to

$$L(k) \hat{u}^+(k) + \hat{u}^-(k) = \frac{\hat{q}(k)}{\omega_-^2(k) - (Vk)^2}, \quad (\text{S22})$$

where superscripts \pm define complex-valued functions which are analytic in the half-planes $\pm \text{Im } k > 0$, respectively. To represent the external DC/AC driving on the boundary of the chain, the function $\hat{q}(k)$ must be chosen to have a zero physical space image $q(\eta) \equiv 0$. The kernel function $L(k) = (\omega_+^2(k) - (Vk)^2) / (\omega_-^2(k) - (Vk)^2)$ has zeros z_j (roots of $\omega_+^2(z_j) = (Vz_j)^2$) and poles p_j (roots of $\omega_-^2(p_j) = (Vp_j)^2$). The symmetry properties $L(-k) = L(k)$ and $L(\bar{k}) = \overline{L(k)}$ remain here the same as in FPU and FK problems. We can then define the sets of poles $P^\pm = P_c^\mp \cup P_r^\pm$ such that $P_c^\pm = \{p : \omega_\pm^2(p) - (pV)^2 = 0, \pm \text{Im } p > 0\}$ and $P_r^\pm = \{p > 0 : \omega_\pm^2(p) - (pV)^2 = 0, \text{Im } p = 0, \pm(\omega'_\pm(p) - V) > 0\}$. Similarly, we define the sets of zeros: $Z^\pm = Z_c^\mp \cup Z_r^\pm$ with $Z_c^\pm = \{z : \omega_\pm^2(z) - (zV)^2 = 0, \pm \text{Im } z > 0\}$ and $Z_r^\pm = \{z > 0 : \omega_\pm^2(z) - (zV)^2 = 0, \text{Im } z = 0, \pm(\omega'_\pm(z) - V) > 0\}$. These poles and zeros are shown in Fig. 9.

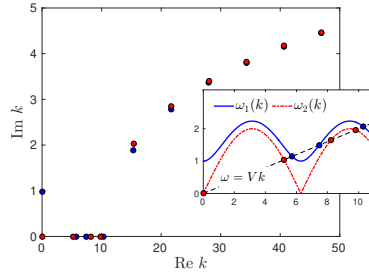


Figure 9: Real and complex zeros (blue markers) and poles (red markers) of the kernel function $L(k)$ for the PB problem. The inset shows the dispersion relation.

The problem (S22) can be solved using the Wiener-Hopf technique [4]. The main step is the factorization of the function $L(k) = L^-(k)/L^+(k)$. The standard factorization formula gives on the real line

$$L^\pm(k) = L^{\mp 1/2}(k) \exp\left(-\frac{1}{2\pi i} \text{p.v.} \int_{-\infty}^{\infty} \frac{\text{Log } L(\xi)}{\xi - k} d\xi\right) \quad (\text{S23})$$

We can alternatively apply the Weierstrass factorization theorem and present the factors as infinite products [4]. Then we obtain the representation

$$L^\pm(k) = \left(\frac{\gamma}{1-V^2}\right)^{\mp 1/2} (0 \mp ik)^{\pm 1} \left[\frac{\prod_{z_j \in Z_r^\pm} (1 - (k/z_j)^2) \prod_{z_j \in Z_c^\pm} (1 - (k/z_j))}{\prod_{p_j \in P_r^\pm} (1 - (k/p_j)^2) \prod_{p_j \in P_c^\pm} (1 - (k/p_j))} \right]^{\mp 1} \frac{1}{S}, \quad (\text{S24})$$

where for future convenience we defined

$$S = \frac{\prod_{z_j \in Z_r^+} z_j \prod_{z_j \in Z_r^-} z_j}{\prod_{p_j \in P_r^-} p_j \prod_{p_j \in P_r^+} p_j}. \quad (\text{S25})$$

These expressions can be evaluated if we know the location of the zeros z_j and the poles p_j introduced above.

We can now rewrite the left hand side of (S22) as a sum of "+" and "-" functions that are analytic in the upper and lower half plane, respectively:

$$\frac{1}{L^+(k)} \hat{u}^+(k) + \frac{1}{L^-(k)} \hat{u}^-(k) = \Psi(k). \quad (\text{S26})$$

The explicit solution of (S26) can be now obtained by decomposing the right hand side

$$\Psi(k) = \frac{1}{L^-(k)} \frac{\hat{q}(k)}{\omega_-^2(k) - (Vk)^2} \quad (\text{S27})$$

into a sum of "+" and "-" functions. To represent the general DC and AC sources we can set

$$\Psi(k) = 2\pi C \delta(k) + 2\pi \sum_{k_j} C_j \delta(k - k_j), \quad (\text{S28})$$

where the wave numbers k_j are chosen from the set Z_r^- if the AC source is located ahead of the defect and from the set P_r^+ if the source is behind the defect. Since $L^-(k_j) [\omega_-^2(k_j) - (Vk_j)^2] = 0$, we have $q(\eta) = 0$ and the sources, parametrized by the constants C (DC driving) and C_j (AC driving), are indeed invisible in the bulk.

If we further additively factorize the delta functions $\delta(k - k_j) = 2\pi [1/(0 + i(k - k_j)) + 1/(0 - i(k + k_j))]$ we can write

$$\Psi(k) = \Psi^+(k) + \Psi^-(k), \quad \Psi^\pm(k) = \frac{C}{0 \mp ik} + \sum_{k_j \in Z_r^- \cup P_r^+} \frac{A_j}{2} \left[\frac{e^{-i(\varphi_j - \pi/2)}}{0 \mp i(k - k_j)} + \frac{e^{i(\varphi_j - \pi/2)}}{0 \mp i(k + k_j)} \right]. \quad (\text{S29})$$

In this representation the complex amplitudes C_j are replaced by the real amplitudes A_j and real phases φ_j . The total number of the corresponding sinusoidal waves is $K = |Z_r^-| + |P_r^+|$.

We can now apply the Liouville theorem [4] to (S26) and obtain the explicit solution of our problem $\hat{u}^\pm(k) = L^\pm(k)\Psi^\pm(k)$. Given that $\hat{u}(k) = \hat{u}^+(k) + \hat{u}^-(k)$ we obtain in the physical space $u(\eta) = \frac{1}{2\pi} \int_{-\infty}^{\infty} L^\pm(k)\Psi^\pm(k)e^{-ik\eta} dk$, when $\pm\eta > 0$, respectively, which gives Eq. 12 and Eq. 13 in the main text. We can now apply the switching condition to obtain $C + \sum_{j=1}^K A_j \sin \varphi_j = u_c$. Then using the boundary condition at $-\infty$ we obtain the link between the constant C and the amplitude of the DC driving τ in the form $\tau = (C/S(V))\sqrt{(1-V^2)/\gamma}$. In the physical space the ensuing solution takes a form $u^\pm(\eta) = u_1^\pm(\eta) + u_2^\pm(\eta)$, for η larger (smaller) than 0, respectively. Here

$$u_1^\pm(\eta) = \sum_{z_j \in Z_r^+/P_r^-} \alpha_j^\pm \cos(z_j\eta + \beta_j^\pm) + \sum_{z_j \in Z_c^+/P_c^-} \alpha_j^\pm e^{-i(z_j\eta + \beta_j^\pm)} \quad (\text{S30})$$

are the terms which do not contain DC/AC driving amplitudes explicitly. However, in contrast to the previous cases, the implicit dependence is present through the real coefficients α_j^\pm and β_j^\pm representing the complex numbers:

$$\alpha_j^\pm e^{-i\beta_j^\pm} = \frac{i\Psi^\pm(k_j)L^\mp(k_j)\gamma}{2k_jV(\omega'_\pm(k_j) - V)}, \quad (\text{S31})$$

where $k_j = z_j$ when the sign is + and $k_j = p_j$ if it is -. The part of the solution explicitly related to external driving can be in turn split into a DC and an AC related parts: $u_2^\pm(\eta) = u_{DC}^\pm(\eta) + u_{AC}^\pm(\eta)$. Here $u_{DC}^+(\eta) = 0$ and

$$u_{DC}^-(\eta) = \frac{C}{S} \sqrt{\frac{1-V^2}{\gamma}} \left[\left(\sum_{z_j \in Z_c^-} \frac{i}{z_j} - \sum_{p_j \in P_c^-} \frac{i}{p_j} \right) - \eta \right]. \quad (\text{S32})$$

The AC related term is

$$u_{AC}^\pm(\eta) = \sum_{k_j \in Z_r^-/P_r^+} A_j |L^\pm(k_j)| \sin(k_j\eta + \varphi_j - \arg L^\pm(k_j)). \quad (\text{S33})$$

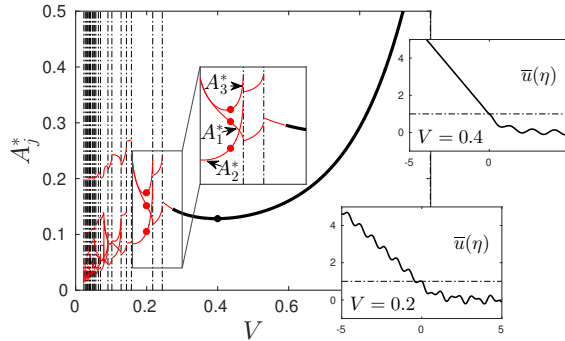


Figure 10: Amplitudes of the AC sources in PB problem: $A_j^*(V)$, $j = 1, 2, \dots, K$. Insets show strains $\bar{u}(\eta) = u(\eta)/u_c$ at $V = 0.2$ and $V = 0.4$ with corresponding A_j^* marked by solid circles. Black lines correspond to admissible solutions, red - to non admissible. Parameters: $\gamma = 1$, $u_c = 1$.

In the main text we showed that in this problem the macro-level energy release rate is $VG^M(V) = (\tau^2(1-V^2)/2 - (\gamma u_c^2)/2)V$ while the rate of dissipation due to the AC driving is:

$$VG^m(V) = \sum_{z_j \in Z_r^-} \frac{A_j^2 |L^+(z_j)|^2}{2} \omega_+^2(z_j) (V - \omega'_+(z_j)) + \sum_{p_j \in P_r^+} \frac{A_j^2 |L^-(p_j)|^2}{2} \omega_-^2(p_j) (\omega'_-(p_j) - V). \quad (\text{S34})$$

The dissipation due to radiated elastic waves is:

$$VG_+(V) = \sum_{z_j \in Z_r^+} \frac{(\alpha_j^+)^2}{2} \omega_+^2(z_j) (\omega'_+(z_j) - V), \quad VG_-(V) = \sum_{p_j \in P_r^-} \frac{(\alpha_j^-)^2}{2} \omega_-^2(p_j) (V - \omega'_-(p_j)). \quad (\text{S35})$$

The validity of the energy balance (S8) in this case was checked numerically for the whole range of velocity $0 < V < 1$.

The total dissipation becomes equal to zero if $\alpha_j^+ = 0$ and $\alpha_j^- = 0$ which can be ensured if we adjust the amplitudes A_j in such a way that $\Psi^+(z_j) = 0$ and $\Psi^+(p_j) = 0$. These conditions can be rewritten as a linear system for the amplitudes A_j :

$$\sum_{k_j \in Z_r^- \cup P_r^+} A_j \frac{k_j^2}{k_j^2 - p_i^2} = u_c, \quad p_i \in P_r^-, \quad \sum_{k_j \in Z_r^- \cup P_r^+} A_j \frac{k_j^2}{k_j^2 - z_i^2} = u_c, \quad z_i \in Z_r^+ \quad (\text{S36})$$

with additional requirement that $\varphi_j = \varphi_j^* = \pi/2$. The variety of solutions of this system is illustrated in Fig. 10.

CRITICAL EXPONENTS

As we mentioned in the main text, the dependence of the velocity of friction-free defects on the amplitude of AC driving shows a supercritical bifurcation which can be interpreted as a continuous (second order) phase transition. The corresponding critical exponents can be evaluated numerically and an interesting question is whether their values show universality.

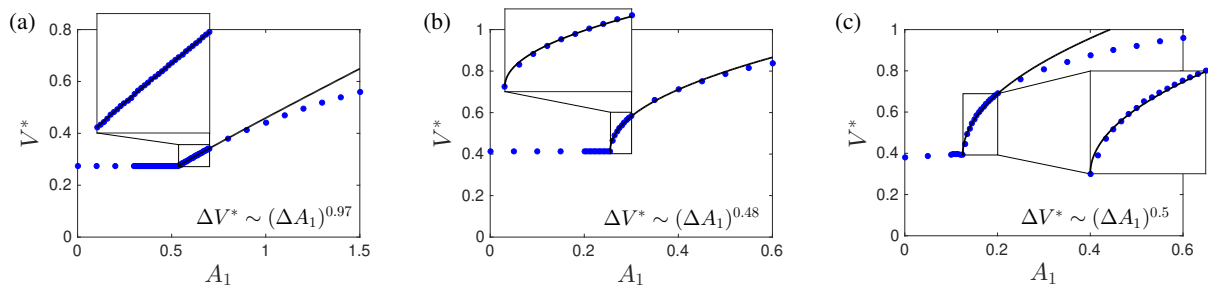


Figure 11: Amplitude dependence of V^* and the corresponding power law fit (solid line): (a) FPU model, (b) FK model, (c) PB model.

In Fig. 11 we reproduced the data for $V^* = V^*(A_1)$ shown in Fig. 2, Fig. 5, and Fig. 7 of the main text. In the same figure we show the obtained asymptotic relations $\Delta V^* \sim \Delta A_1^r$ where $\Delta V^* = V^* - V^*(0)$ and $\Delta A_1 = A_1 - A_1^0$. In the case of FK model and PB model the computed values of the exponent r stay very close to 0.5 corresponding to mean field Landau theory and hinting towards universality. Instead, in the case of FPU model the value of the exponent r is closer to 1.0 which suggests a link with mean field depinning [5]. The presence of the two classes may be due to the fact that in FPU models the problem is quasi-linear (nonlinearity concerns the (discretized) derivatives) while in both FK and PB models the problem is semilinear (nonlinearity concerns the function itself). A potentially important signature of this difference is that in FPU model of relevance is the dispersion of the acoustic branch while in both FK and PB models the main role is played by the dispersion of the optical branch.

-
- [1] L. Truskinovsky and A. Vainchtein, *SIAM Journal on Applied Mathematics* **66**, 533 (2005).
 - [2] N. Flytzanis S. Crowley and V. Celli, *Journal of Physics and Chemistry of Solids* **38**, 539–552 (1977).
 - [3] A. Vainchtein, *Journal of the Mechanics and Physics of Solids* **58**, 227–240 (2010).
 - [4] B. Noble, *Methods based on the Wiener-Hopf technique for the solution of partial differential equations* (1958).
 - [5] D. S. Fisher, *Physics reports* **301**, 113–150,(1998).